Biochimica et Biophysica Acta, 1020 (1990) 253–259
Elsevier

BBABIO 43303

Time-resolved FTIR spectroscopy of quinones in *Rb. sphaeroides* reaction centers

D.L. Thibodeau [1], E. Nabedryk [1], R. Hienerwadel [2], F. Lenz [2], W. Mäntele [2] and J. Breton [1]

DBCM, CEN Saclay, Gif-sur-Yvette (France)
and [2] Institut für Biophysik und Strahlenbiologie, Universität Freiburg, Freiburg (F.R.G.)

(Received 18 June 1990)

Key words: Time resolved spectroscopy; Infrared spectroscopy; Photosynthesis; Quinone; Bacterial reaction center; Reaction center; (*Rb. sphaeroides*)

Light-induced intermediates in reaction centers of *Rhodobacter sphaeroides* have been investigated by time-resolved Fourier transform infrared (FTIR) difference spectroscopy with a time-resolution of 25 ms at a spectral resolution of 4 cm^{-1}. Following photoexcitation, an electron is rapidly transferred from the primary donor (P) to acceptor quinones, Q_A and Q_B. Based on the different recombination lifetimes of the photoinduced intermediates (60–100 ms for $P^+Q_A^- \rightarrow PQ_A$ and a few seconds for $P^+Q_AQ_B^- \rightarrow PQ_AQ_B$), a comparison between the $P^+Q_A^-$-minus-PQ_A ($P^+Q_A^-/PQ_A$) and $P^+Q_AQ_B^-$-minus-PQ_AQ_B ($P^+Q_AQ_B^-/PQ_AQ_B$) spectra becomes reliable, since both difference spectra are measured: (i) for the same sample, (ii) at the same temperature, (iii) in the same chemical environment, (iv) from the same actinic event, and (v) with the same background. For the first time, the small variations observed between the two difference spectra, $P^+Q_A^-/PQ_A$ and $P^+Q_AQ_B^-/PQ_AQ_B$, have been interpreted in terms of contributions from only Q_A, Q_B^-, Q_A^-, Q_B and their amino acid partners without the interference from P and P^+. Vibrational modes ascribed to neutral quinone carbonyls could not be singled out, instead several bands were related to changes in interaction of amino acid residues with Q_A and Q_B following photoexcitation. In particular, three bands (1670 cm^{-1}, 1652 cm^{-1}, 1630 cm^{-1}) insensitive to ^1H–^2H exchange have been identified. The feature at 1670 cm^{-1} was not apparent in previous steady-state studies, the 1652^{-1} band has been associated to a conformational change of the peptide C=O of the conserved Ala M260 residue in the Q_A pocket. The 1493 cm^{-1}, 1480 cm^{-1} (Q_B^-) and the 1460 cm^{-1} (Q_A^-) bands have been revealed and attributed to C=C vibrations of the semiquinone anion without excluding the possibility of some C–O^- contributions. The 1732 cm^{-1}, 1555 cm^{-1}, and 1533 cm^{-1} bands can be assigned to amino acid vibrations. The band at 1555 cm^{-1} could reflect the effect of the Q_A delocalized charge on the ring of Trp M252 in van der Waals contact with Q_A.

Introduction

Primary photosynthetic reactions feature rapid kinetics with high quantum yield of stable charge separation occurring in basic units called reaction centers (RC). Typically, purple bacterial RC contain four bacteriochlorophylls (BChl), two bacteriopheophytins (BPhe), two unequivalent quinones, one of which (Q_A) is more tightly bound to the protein than the other one (Q_B), and a non-heme iron. In *Rhodobacter (Rb.) sphaeroides* RC, Q_A and Q_B are both ubiquinones (UQ) but display different properties (e.g., Q_A is a one-electron acceptor while Q_B can accept two electrons under physiological conditions). Following photoexcitation, the electron is transferred from the primary donor (a dimer of BChl), P, to the primary acceptor quinone, Q_A, in 200 ps. When the loosely bound quinone Q_B is present in the RC the electron transfer from Q_A to Q_B takes place in approx. 100 μs at room temperature. In the absence of an extrinsic electron donor to P^+, the $P^+Q_A^-$ state has a lifetime in the 60-to-100 ms range while $P^+Q_AQ_B^-$ lasts a few seconds, at room temperature [1]. At 100 K, the recombination half-life of $P^+Q_A^-$ is 30 ms [1] and the electron is no longer transferred from Q_A to Q_B [2].

Abbreviations: FTIR, Fourier transform Infrared; P, primary donor; RC, reaction centers; BChl, bacteriochlorophyll; BPhe, bacteriopheophytin; Q_A, primary acceptor quinone; Q_B, secondary acceptor quinone; *Rb., Rhodobacter*; UQ, ubiquinone; TR, time-resolved; PS II, Photosystem II; a.u., absorbance unit.

Correspondence: D.L. Thibodeau, SBE, DBCM, Bât. 532, CEN Saclay, 91191 Gif-sur-Yvette Cedex, France.

Recent X-ray crystallographic data of bacterial RC [3–5] suggest that the efficiency and stability of charge separation rely at least partially on the protein environment to optimize the orientation and the localization of the various redox components involved in electron transport. More specifically, differences in the nature and organization of the amino acids forming the binding pocket of Q_A and Q_B might explain the different redox properties of the two quinones. However, X-ray studies, which yield essentially a static picture of the atomic structure of the RC in their relaxed state, have yet to provide information on light-induced structural changes. Infrared (IR) spectroscopy, which is very sensitive to small alterations of bond energies, therefore represents an attractive method to follow the structural and functional changes in the RC at the level of individual groups of the protein and cofactors. The importance of Fourier transform IR (FTIR) difference spectroscopy in elucidating the structure and dynamics of membrane proteins have been recently reviewed [6].

Structural changes which accompany the formation of the states $P^+Q_A^-$ and $P^+Q_AQ_B^-$ in *Rb. sphaeroides* RC have been previously characterized under steady-state illumination conditions using light-induced FTIR difference spectroscopy [7–10]. By comparison of the $P^+Q_A^-$-minus-PQ_A ($P^+Q_A^-/PQ_A$) and $P^+Q_AQ_B^-$-minus-PQ_AQ_B ($P^+Q_AQ_B^-/PQ_AQ_B$) spectra with those obtained by electrochemically-generated BChl cation [8] and semiquinone anion [11] species, the light-induced FTIR spectra in the C=O frequency range appear clearly dominated by the contribution from P^+ and P. Under steady-state conditions, a comparison between $P^+Q_A^-/PQ_A$ and $P^+Q_AQ_B^-/PQ_AQ_B$ spectra necessarily implies either the comparison of different samples (e.g., RC containing only Q_A, or both Q_A and Q_B, or RC with isotopically-labelled quinones [9]) or different temperature conditions [9,10]. Under these conditions, the contribution from the Q_A and Q_B functional groups (C=O and C=C) and their surrounding amino acid residues affected during the photoreduction have been proven difficult to detect.

Vibrational studies of transient systems with simultaneous temporal and spectral resolution can provide detailed information on rate constants and population distribution of intermediates or products. Time-resolved (TR) FTIR difference spectroscopy has been recently applied to biological systems such as rhodopsin [12] or bacteriorhodopsin [13–15]. The most attractive attribute of TRFTIR difference spectroscopy is that it is possible to record information on transient states simultaneously on all the IR spectral range. In this study, TRFTIR difference spectroscopy was implemented as a new strategy for the study of quinones following photoexcitation in bacterial RC with a time-resolution of 25 ms for a spectral resolution of 4 cm^{-1} [16]. The signal components of $P^+Q_A^-/PQ_A$ and $P^+Q_AQ_B^-/PQ_AQ_B$ spectra can be discriminated using the same sample at the same temperature based on their temporal properties. For the first time, the small variations observed between the two difference spectra, $P^+Q_A^-/PQ_A$ and $P^+Q_AQ_B^-/PQ_AQ_B$, have been interpreted in terms of contributions from only Q_A, Q_B^-, Q_A^-, Q_B and their amino acid partners without the interference from P and P^+.

Materials and Methods

The secondary acceptor quinone is partially lost upon isolation and purification of the *Rb. sphaeroides* RC. The Q_A-to-Q_B electron transfer can be recovered by addition of an excess of UQ [1,17]. UQ-6 (Sigma) was solubilized first in dimethyl sulfoxide then added to a 10% deoxycholate solution. Up to 80% reconstitution of functional Q_B in its site was achieved by addition of a 30-fold excess of UQ-6 to the isolated RC (0.5% cholate/NaCl). The solution volumes were adjusted so that the final concentration of dimethyl sulfoxide and deoxycholate never exceeded 2%. The RC-quinone samples were left on ice for 90 min, then washed once with 5 mM ascorbate solution and subsequently with several aliquots of distilled water, between each addition they were re-concentrated by ultrafiltration (Centricon-30, Amicon) to reduce the detergent concentration. Samples in ^2H_2O were prepared by substituting ^2H_2O for H_2O in the washing steps. The extent of the Q_B reconstitution was evaluated by the kinetics of absorbance changes performed in the near-IR at 960 nm. Air-dried films of RC on CaF_2 discs were rehydrated with H_2O (or ^2H_2O) vapor before the FTIR measurements. The IR absorbance at the peak of the amide I band was kept below 0.8 absorbance units (a.u.). Light-induced FTIR spectra were obtained under continuous illumination prior to TRFTIR experiments to check the integrity of the samples and to monitor the time necessary to complete the back-reaction from $P^+Q_AQ_B^-$ to PQ_AQ_B, since this recombination time is sensitive to both sample hydration and temperature.

FTIR measurements were performed on a Nicolet 60SX spectrometer equipped with a MCT-A detector. The spectrometer is able to perform Rapid Scan, a term which refers to the acquisition and storage of a large number of interferograms in a brief period of time. The Rapid Scan method implies that the mirror moves smoothly and rapidly (typically 3 cm/s) while the time-dependent data are recorded. The time resolution is limited by the maximum digitization rate of the analog-to-digital converter and the velocity of the mirror [18]. Data collection was performed by using unidirectional mode to yield a time resolution of 25 ms at 4 cm^{-1} spectral resolution. The timing of events was under the control of the logical level of the signal of the Nicolet 60SX computer. The only additional circuit is an elec-

tronic device which provides a logic signal that indicates the start of the first scan. Since Fourier transform cannot be performed quickly, unprocessed interferograms are stored on the computer. Fig. 1 shows a timing diagram of the Rapid Scan experiment. Ten consecutive interferograms are recorded in approx. 2 s. Each interferogram, digitized over 2560 data points, of which 295 are digitized before the peak of the interferogram, contains information corresponding to a mid-IR spectrum [18]. The logic pulse is used to trigger a shutter after a suitable delay (approx. 1 s). When the shutter is open, a filtered (2.5 cm of water and one RG715) 150W-projector lamp illuminates the sample for 100 ms while interferogram 3 (Fig. 1) is recorded. Under light-saturating conditions, $P^+Q_A^-$ (100 K) or both $P^+Q_A^-$ and $P^+Q_AQ_B^-$ (280 K) species are produced and they decay with their respective lifetime as soon as the shutter is closed. Because extensive signal averaging was necessary to detect the small absorbance changes by difference spectroscopy, the cycle of recording ten interferograms was repeated several hundred times and the interferograms corresponding to the same time-delay were co-added. The repetition rate between two actinic events was set at several tens of seconds (typically 50 s) to ensure complete relaxation of the RC to the ground state. After

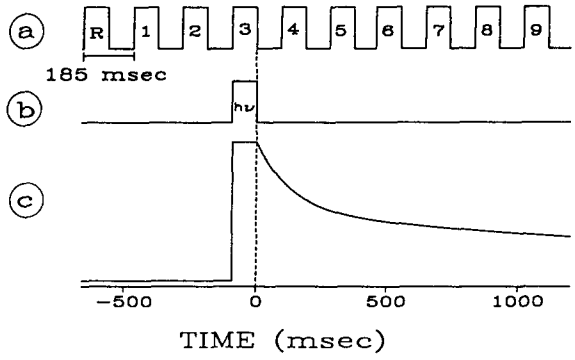

Fig. 1. Timing diagram of one cycle of the Rapid Scan experiment. (a) The boxcar function represents the consecutive digitization of ten interferograms. The first single-beam (R) of the series is taken as a reference on which every subsequent single-beam will be ratioed. Cycles are spaced by 50 s and repeated several hundred times. (b) The actinic event (100 ms) is delayed from the start of the series of data collection to occur at the beginning of the digitization of interferogram 3. (c) The trace represents the concentration of the $P^+Q_A^-$ and $P^+Q_AQ_B^-$ transient species at 280 K produced under light-saturating conditions, the complex decay curve shows the combination of their respective lifetime.

Fourier transform, ten single-beam spectra spaced every 185 ms were obtained. To produce the nine difference absorption spectra shown in Fig. 2, each one of the

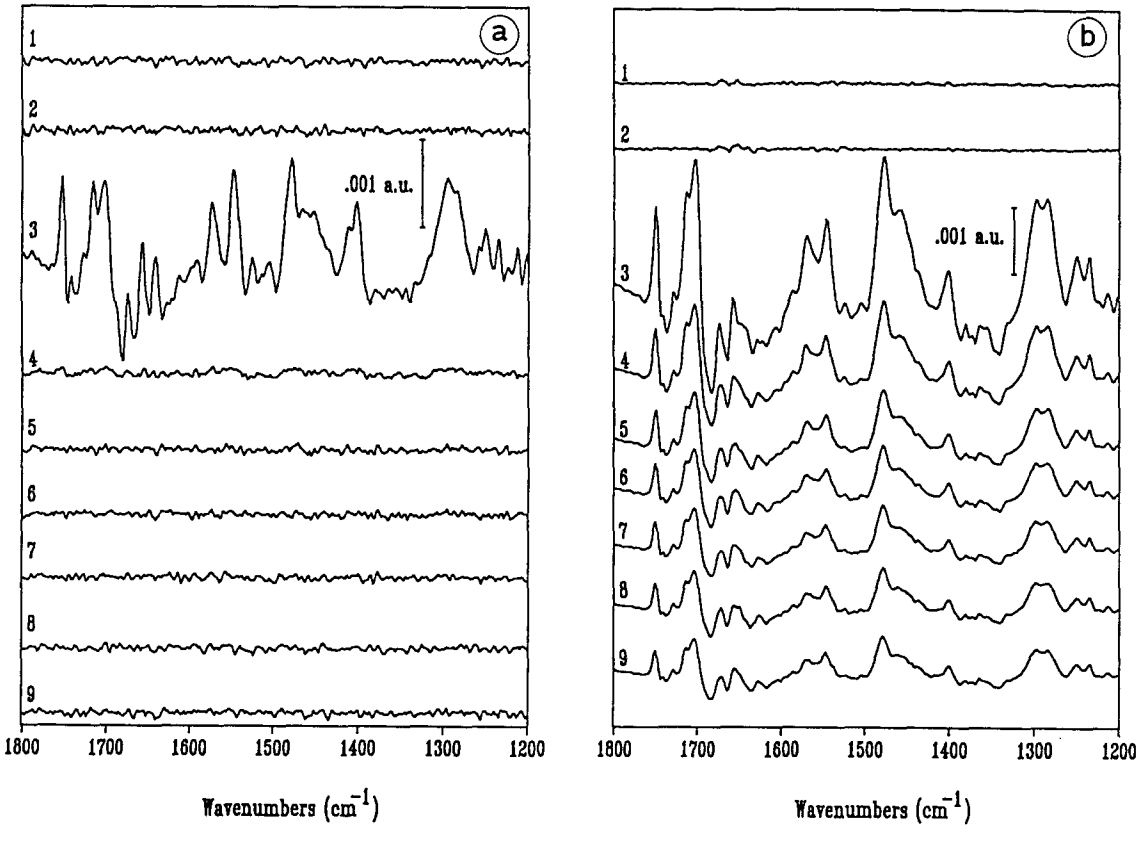

Fig. 2. Series of time-resolved FTIR difference spectra of *Rb. sphaeroides* reaction centers at (a) 100 K and (b) 280 K. The time-resolved difference spectra (co-addition of 1540 interferograms) are separated by 185 ms. Spectrum 3 in each series is recorded during illumination (100 ms) of RC. a.u.: absorbance unit.

series of ten single-beam spectra was ratioed against the reference single-beam spectrum (R in Fig. 1a). After 8–24 hours of signal-averaging, the noise is reduced to $\leqslant 5 \cdot 10^{-4}$ a.u. in the 1800-to-1200-cm^{-1} region. TRFTIR difference spectra corresponding to the $PQ_A \rightarrow P^+Q_A^-$ and $PQ_AQ_B \rightarrow P^+Q_AQ_B^-$ transitions in *Rb. sphaeroides* RC have been obtained with a S/N comparable to the steady-state difference spectra [9,10]. The band frequencies are considered to be accurate to ± 1 cm^{-1}.

Results

Figs. 2a and 2b show two typical series of nine successive TRFTIR difference spectra acquired with *Rb. sphaeroides* RC at 100 K and 280 K, respectively, in a Rapid Scan experiment. These TRFTIR difference spectra, each separated by 185 ms, can be classified into three groups: (i) before illumination, (ii) during the 100 ms illumination, (iii) after illumination. In Fig. 2, starting from the top, there are: (i) the two first difference spectra which provide background (dark-minus-dark) spectra, (ii) the third spectrum which is similar in band frequencies and amplitudes to that obtained under steady-state illumination [8–10], (iii) the subsequent spectra which reflect the concentration of the transient species. At 100 K, the electron transfer from Q_A to Q_B is blocked [2], implying that only the decay of $P^+Q_A^-$ species can be observed at this temperature. This is clearly shown in Fig. 2a: a transient spectrum is obtained only during the 100 ms illumination while the rest of the series displays negligible contribution. This demonstrates that the transient species have completely decayed within 100 ms after illumination and thus before the start of the next data acquisition. Fig. 2b shows the analogous experiment at 280 K where electron transfer proceeds from Q_A^- to Q_B. The spectrum under illumination contains, at this temperature (spectrum 3 in Fig. 2b), contributions of $P^+Q_A^-$ and $P^+Q_AQ_B^-$ transient species and their relaxed states. Since $P^+Q_AQ_B^-$ decays with a much longer lifetime, this transient state subsists in the difference spectra after the $P^+Q_A^-$ has decayed.

Fig. 3 shows the amplitude of several transient IR absorbance bands observed in Fig. 2b as a function of time. Each band of the spectrum under illumination was normalized to 1. The slope of the plot reflects the presence of a biphasic decay with $t_{1/2}$ of 90 ± 2 ms and 1.8 ± 0.2 s, in good agreement with the known $t_{1/2}$ of 60–100 ms for $P^+Q_A^-$ and a few seconds for $P^+Q_AQ_B^-$ [1]. By analyzing the charge recombination kinetics into fast and slow phases, the relative proportion of photochemically-active $P^+Q_A^-$ and $P^+Q_AQ_B^-$ were determined. The $P^+Q_AQ_B^-/PQ_AQ_B$ spectrum is calculated from the average of the last four spectra from Fig. 2b; typically all the spectra recorded 500 ms after the end of the illumination show that the $P^+Q_A^-$ species no longer contributes to the spectra at 280 K (Fig. 3, dotted line). The initial amplitude of $P^+Q_AQ_B^-/PQ_AQ_B$ is estimated by the coefficient of the slow phase in the two-exponential fit. The $P^+Q_A^-/PQ_A$ spectrum (Fig. 4b, dashed line) obtained at 280 K by TRFTIR spectroscopy, is the result of the subtraction of the spectrum recorded under illumination (spectrum 3 of Fig. 2b) and the calculated $P^+Q_AQ_B^-/PQ_AQ_B$ spectrum. Similar S/N for both calculated difference spectra is desirable to facilitate their comparison. To that effect the contribution of $P^+Q_A^-/PQ_A$ should be ideally twice that of $P^+Q_AQ_B^-/PQ_AQ_B$ under illumination, since the averaging of four $P^+Q_AQ_B^-/PQ_AQ_B$ spectra leads to a 2-fold improvement in S/N. To approach the ideal proportion of each

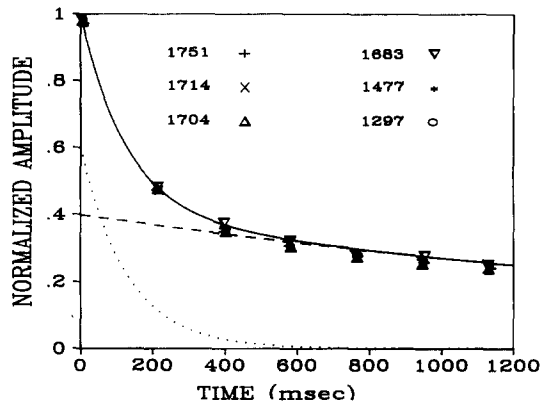

Fig. 3. Changes in amplitude at several IR wavenumbers from the data shown in Fig. 2b as a function of time. The solid line is the least-squares fit according to the function: $A(t) = A_0 \cdot \exp(-\ln 2 \cdot t/t_A) + B_0 \cdot \exp(-\ln 2 \cdot t/t_B)$, where A_0 and B_0, the initial concentrations of $P^+Q_A^-/PQ_A$ and $P^+Q_AQ_B^-/PQ_AQ_B$ are (60 ± 2)% and (40 ± 2)%, respectively, and t_A and t_B are, (90 ± 3) ms and (1.8 ± 0.2) s. These parameters are used to construct the two decay curves of $P^+Q_A^-/PQ_A$ (dotted line) and $P^+Q_AQ_B^-/PQ_AQ_B$ (dashed line).

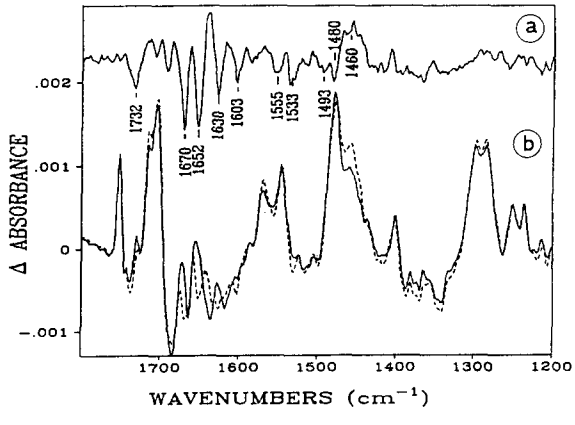

Fig. 4. Time-resolved FTIR difference spectra of *Rb. sphaeroides* reaction centers. (a) The Q_A-$Q_B/Q_AQ_B^-$ spectrum is obtained from the subtraction of P^+Q_A-$/PQ_A$ and $P^+Q_AQ_B$-$/PQ_AQ_B$ normalized from decay parameters shown in Fig. 3 or on the 1750 cm^{-1} band. (b) Difference spectra calculated and normalized from data shown in Fig. 2b both obtained during the same measurement series at 280 K. $P^+Q_A^-/PQ_A$ (dashed line), $P^+Q_AQ_B^-/PQ_AQ_B$ (solid line).

transient states, the mixed population of RC with functional and non-functional Q_B sites was controlled by partial reconstitution of the Q_B content in the RC and by adjustment of the temperature. Samples with various amounts of Q_B (0–80%) have been used to check that incorporation of UQ-6 did not affect the results of TRFTIR difference spectroscopy: samples with 0%, 30%, and 80% Q_B all yielded similar time-resolved $P^+Q_A^-/PQ_A$ spectra, which themselves were comparable to those obtained under steady-state conditions. The dashed line in Fig. 3 shows that $P^+Q_AQ_B^-/PQ_AQ_B$ is estimated to 40% of the signal amplitude obtained under illumination for the data shown in Fig. 2b. In Fig. 4b, the respective amplitudes of $P^+Q_A^-/PQ_A$ and $P^+Q_AQ_B^-/PQ_AQ_B$ spectra have been normalized for purpose of comparison by two methods yielding similar results: (i) by data processing using the fit parameters (from Fig. 3) for the exponential decay of the two species or (ii) by matching the 1750 cm^{-1} band, which corresponds to the contribution of mostly P^+/P [8], from each difference spectrum.

At first sight, the two calculated spectra ($P^+Q_A^-/PQ_A$ and $P^+Q_AQ_B^-/PQ_AQ_B$) are very much alike, an observation which is consistent with earlier results obtained by steady-state FTIR difference spectroscopy [9,10]: the P^+/P absorbance bands dominate the TRFTIR difference spectra of RC. Nonetheless, small variations between the $P^+Q_A^-/PQ_A$ and $P^+Q_AQ_B^-/PQ_AQ_B$ difference spectra can be noticed especially in the 1675-to-1600 cm^{-1} region where the C=O and C=C modes of quinones could contribute. Fig. 4a shows the subtraction of the normalized $P^+Q_A^-/PQ_A$ and $P^+Q_AQ_B^-/PQ_AQ_B$ spectra. The resulting spectrum is denoted $Q_A^-Q_B/Q_AQ_B^-$ to stress that the contributions of P and P^+ have been cancelled assuming that the signal of P^+/P is the same whether the quinone acceptor is Q_A or Q_B. It is important to keep in mind that in this $Q_A^-Q_B/Q_AQ_B^-$ spectrum (Fig. 4a) the positive bands contain contributions of neutral Q_B or charged Q_A^- while the negative features represent contributions originating from neutral Q_A or charged Q_B^-. In addition, amino acid partners of Q_A and Q_B could also contribute to the $Q_AQ_B/Q_AQ_B^-$ spectrum. In particular, three negative bands have been identified in the C=O region, notably the band at 1670 cm^{-1} which was not apparent in previous steady-state studies, and two bands at 1652 cm^{-1} and 1630 cm^{-1}. Furthermore, other bands have been revealed of which the negative 1603 cm^{-1}, 1493 cm^{-1}, 1480 cm^{-1} and the positive $\approx$ 1460 cm^{-1} are in region of C=C, C=C, and/or $C-O^-$ quinone vibrations, whereas the 1732 cm^{-1}, 1555 cm^{-1}, 1533 cm^{-1} bands can be assigned to amino acid vibrations.

Discussion

The quinone carbonyl vibrational modes have been found surprisingly small and difficult to pinpoint in steady-state FTIR spectra [9,10,19] owing to the masking effect of the large contribution of P and P^+ in the light-induced difference spectra. The TRFTIR difference spectroscopy technique presented here was developed to reveal the vibrational contributions of the quinones Q_A and Q_B and their binding sites. The distinct decay lifetime of the $P^+Q_A^-$ and $P^+Q_AQ_B^-$ transient species is the key element on which the TR FTIR technique discriminates the contributions of $P^+Q_A^-/PQ_A$ and $P^+Q_AQ_B^-/PQ_AQ_B$. The subtraction of these two difference spectra was performed to isolate absorbance changes ascribed to the quinones from the interference of bands originating from the primary donor.

Absorbance changes reflecting quinone contributions are caused by two main effects. A direct effect will appear as changes in the bond energies of the quinone itself (most likely C=O, C=C stretching): Q_A or Q_B after accepting an electron has a net charge that affects the strength of bonds and thus their vibrational modes. Direct effects could be monitored by reconstitution of RC with, either quinones that absorb at different frequencies (e.g., duroquinone), or their ^{13}C and ^{18}O isotopomers [9] where a C=O and C=C frequency downshift is expected. An indirect effect is invoked when amino acid residues are affected rather than the quinones themselves. To first order, we anticipate that amino acids interacting directly with the quinones would respond to local changes of the electrostatic environment, even though it cannot be excluded that amino acid residues at a distance from the quinone protein pocket might also contribute.

The polarizability and the ionizability of the amino acid groups that form the lining of the quinone pockets are the two major properties that are considered to explain the differences in the environment for the two quinones. The elucidation of the X-ray structure of bacterial RC has revealed a detailed picture of the quinone-protein interactions [3–5] which can be classified in terms of (i) hydrogen bonding, (ii) aromatic ring interactions, and (iii) van der Waals contact. An important difference between the binding sites of Q_A and Q_B is the more polar nature of the Q_B site owing to the several ionizable residues located near Q_B. More specifically, in *Rb. sphaeroides* RC, Glu L212 (conserved in all bacteria and plant systems) and Asp L213 are in van der Waals contact with the Q_B ring, while Asp L210, Arg L217, Glu H173 and all five residues ligated to Fe are within 10 Å of Q_B [4]. In contrast, no ionizable residues other than the His ligated to Fe are located within 8 Å of the Q_A ring, although two are found within 10 Å (Glu L104 near $BPheo_L$ and Glu M234 near Fe). Several aromatic residues are located near Q_A. In particular, the aromatic ring of Trp M252 which is nearly parallel to the Q_A ring and makes van der Waals contacts to both Q_A and Phe M251. In addition, this

Trp residue which is conserved in bacteria and plant systems bridges $BPheo_L$ and Q_A. The aromatic ring of Phe L216 near Q_B is symmetry-related to Trp M252 near Q_A but does not make van der Waals contact with Q_B [4]. X-ray data of *Rb. sphaeroides* RC [4], also indicate that the two carbonyl oxygens of Q_A are within hydrogen-bonding distance to the peptide nitrogen of Ala M260 and the side-chain of Thr M222, respectively, whereas the carbonyls of Q_B are within hydrogen-bonding distance to the imidazole ring of His L190 and the side-chain of Ser L223 (a conserved residue in all bacterial and plants RC). From in situ midpoint potential measurements, it has also been shown that the interaction strength of the Q_A semiquinone in its site is considerably enhanced compared to the neutral quinone [20]. The hydrogen-bond lengths determined by ENDOR spectroscopy for Q_A^- are 1.55 Å and 1.78 Å [21].

The assignments of the signals obtained by TRFTIR difference spectroscopy are made on the basis of the direct and indirect effects. More specifically in the 1600-to-1700 cm^{-1} C=O stretching region, three negative bands are observed at 1670 cm^{-1}, 1652 cm^{-1} and 1630 cm^{-1}. These frequencies indicate that the bands arise from either the neutral Q_A carbonyls or amino acid residues interacting with Q_A or Q_B. The attribution to the carbonyls of Q_B^- can be easily excluded, since IR spectroelectrochemical studies of UQ model-compounds have shown that the $C-O^-$ from the semiquinone anion shows up in the 1500-to-1475 cm^{-1} range [11 and references therein]. Previous steady-state FTIR studies of the $P^+Q_A^-/PQ_A$ spectrum of *Rb. sphaeroides* have revealed a negative band at 1650 cm^{-1} assigned to a peptide C=O group, since it does not shift upon reconstitution of RC with duroquinone, or ^{18}O-UQ-10, or ^{13}C-UQ-10 at the Q_A site [9]. The 1650-1 band, which is unique to the $P^+Q_A^-/PQ_A$ spectrum, was interpreted in terms of a conformational change of the protein backbone, possibly at the conserved Ala M260 residue of the Q_A binding pocket. Indeed TRFTIR difference spectra (Fig. 4) reinforce that the ≈ 1650 cm^{-1} band belongs to the $Q_A \rightarrow Q_A^-$ transition. As well, TRFTIR difference spectra reveal an additional feature at 1670 cm^{-1} not detected in steady-state spectra. The band at 1630 cm^{-1} is also a candidate for a Q_A-carbonyl group, although it is downshifted by ≈ 30 cm^{-1} with respect to the frequency observed for quinone model-compounds in vitro [11], a possibility that cannot be excluded in view of the Q_A environment specificity [4]. The three negative bands (1670 cm^{-1}, 1652 cm^{-1}, 1630 cm^{-1}) are insensitive to ^2H_2O exchange (data not shown), although a study as a function of p^2H has yet to be completed. In agreement with steady-state spectra [9], the 1603 cm^{-1} band in Fig. 4a can be assigned to the C=C of Q_A. In the frequency region of the semiquinone $C-O^-$ and C=C vibrations, two negative bands at 1493 cm^{-1} and 1480 cm^{-1} and a positive band at ≈ 1460 cm^{-1} are observed (Fig. 4a). Preliminary experiments with Q_A and Q_B replaced by their ^{13}C isotopomers reveal that the complex negative band at 1493–1480 cm^{-1} shifts to a broad band centered at 1434 cm^{-1}. This initial result indicates that the negative bands associated with Q_B^- and the positive ones with Q_A^- could arise from C=C vibrations of the semiquinone anions without excluding the possibility of $C-O^-$ contributions. The 1670 cm^{-1} and 1652 cm^{-1} negative bands remain at the same position when Q_A and Q_B are replaced by their ^{13}C isotopomers; accordingly these bands cannot be attributed to neutral quinone-carbonyl vibrations but most probably to amino acids in interaction with Q_A and Q_B. In Fig. 4a, the negative bands at 1555 cm^{-1} and 1533 cm^{-1} are revealed by TRFTIR difference spectroscopy in a frequency range representative of vibrations in the amide II band. One of these bands could originate from the NH peptide group of the Ala M260 residue of the Q_A pocket and could be correlated to the corresponding change in the amide I region at 1652 cm^{-1}. Another possibility would be the involvement of the Trp M252 ring vibration, since this residue is in van der Waals contact with Q_A. The centers of Q_A, Trp M252 and Phe M251 lie approx. on a straight line. The presence of a negative charge on Q_A is expected to alter the Trp ring mode and would lead to the rise of the 1555 cm^{-1} or 1533 cm^{-1} signal in the $Q_A^-Q_B/Q_AQ_B^-$ spectrum. Above 1700 cm^{-1} negative signal lies in the frequency range of carbonyl of protonated carboxylic groups and could involve an absorption change of a Glu or Asp side-chain in the Q_B binding pocket or near the Q_A site. Recent experiments on *Rb. sphaeroides* RC, involving the comparison between the electrochemically-generated P cation and the photochemically charge-separated $P^+Q_A^-$ state [22], lead to a Q_A^-/Q_A spectrum which presents several analogies with the $Q_A^-Q_B/Q_AQ_B^-$ spectrum displayed on Fig. 4a. This reinforces the assignments of the 1732 cm^{-1}, 1670 cm^{-1} 1652 cm^{-1}, 1630 cm^{-1}, 1555 cm^{-1} and 1533 cm^{-1} bands to the $Q_A \rightarrow Q_A^-$ transition. In particular, the observation of a signal at 1732 cm^{-1} (which most probably originates from a residue outside the Q_A pocket) suggests that amino acid side-chains away from the quinone protein pocket might be perturbed upon photoreduction of Q_A and contribute to the FTIR difference spectrum. Analogies between bacteria and Photosystem II (PS II) in plants are also observed in the carbonyl frequency region, especially at 1670 cm^{-1}, as well as in the 1560-to-1550 cm^{-1} domain [23]. These signals common to the FTIR spectra of the primary quinone photoreduction in both bacteria and plants bring additional evidence that some amino acid-Q_A interactions are conserved in PS II, in agreement with significant sequence homologies between amino acid sequences of M and D2 polypeptides [24,25] and with modelling experiments on the plastoquinone bind-

ing site in PS II. In particular, the conserved Trp residue located near Q_A (Trp D2-254 in PS II is analogous to Trp M252 in bacterial RC) could lead to the differential signal observed at 1560/1550 cm^{-1} in PS II and at 1555 cm^{-1} in *Rb. sphaeroides* RC.

Because all spectral elements in the region of interest are recorded simultaneously, TRFTIR difference spectroscopy studies are advantageous to define the mode frequencies of interest for kinetic IR studies at individual wavelengths which can follow electron transfer steps at time resolutions that are not accessible by Rapid Scan difference spectroscopy. An IR-diode-laser system capable of microsecond time-resolution described in Ref. 26 has been used to follow the rise and decay of selected bands (unpublished data). The bands at 1480 cm^{-1} and 1493 cm^{-1}, which have been attributed to Q_B^- in this study, both display the characteristic rise of the electron transfer from Q_A^- to Q_B (100–150 μs) and of the recombination decay of $P^+Q_AQ_B^- \rightarrow PQ_AQ_B$ (approx. 2 s). Indeed, TRFTIR difference spectroscopy opens a new dimension for future experiments in vibrational spectroscopy of photosynthetic systems.

Acknowledgements

Part of this work was supported by EEC (ST2J-O118-2-D). *Rb. sphaeroides* RC reconstituted with [^{13}C]ubiquinones were kindly provided by K.A. Bagley, M.Y. Okamura and G. Feher (La Jolla, U.S.A.). J.B. and D.L.T. thank K. Gerwert for enlightening discussions. D.L.T. gratefully acknowledges support from Ministère des Affaires Etrangères de France and NATO/NSERC for a post-doctoral fellowship.

References

1 Clayton, R.K. and Yau, H.F. (1972) Biophys. J. 12, 867–881 Codgell, J.R., Brune, D.C. and Clayton, R.K. (1974) FEBS Lett. 45, 344–347.
2 Parson, W.W. (1978) in The Photosynthetic Bacteria (Clayton R.K. and Sistrom W.R., eds.), pp. 455–469, Plenum, New York.
3 Michel, H., Epp, O. and Deisenhofer, J. (1986) EMBO J. 5, 2445–2451.
4 Allen, J.P., Feher, G., Yeates, T.O., Komiya, H. and Rees, D.C. (1988) Proc. Natl. Acad. Sci. USA 85, 8487–8491.
5 Deisenhofer, J. and Michel, H. (1989) EMBO J. 8, 2149–2170.
6 Braiman, M.S. and Rothschild, J.K. (1988) Annu. Rev. Biophys. Biophys. Chem. 17, 541–570.
7 Mäntele, W.G., Nabedryk, E., Tavitian, B.A., Kreutz, W. and Breton, J. (1985) FEBS Lett. 187, 227–232.
8 Mäntele, W., Wollenweber, A., Nabedryk, E. and Breton, J. (1988) Proc. Natl. Acad. Sci. USA 85, 8468–8472.
9 Bagley, K.A., Abresch, E., Okamura, M.Y., Feher, G., Bauscher, M., Mäntele, W., Nabedryk, E. and Breton, J. (1990) in Current Research in Photosynthesis (Baltscheffsky M., ed.), Vol. I, pp. 77–80, Kluwer, Dordrecht.
10 Nabedryk, E., Bagley, K.A., Thibodeau, D.L., Bauscher, M., Mäntele, W. and Breton, J. (1990) FEBS Lett. 266, 59–62.
11 Bauscher, M., Nabedryk, E., Bagley, K. A., Breton, J. and Mäntele, W. (1990) FEBS Lett. 261, 191–195.
12 Rothschild, K.J., Gillespie, J. and DeGrip, W.J. (1987) Biophys. J. 51, 345–350.
13 Braiman, M.S., Ahl, P.L. and Rothschild, K.J. (1987) Proc. Natl. Acad. Sci. USA 84, 5221–5225.
14 Gerwert, K. and Hess, B. (1988) Mikrochim. Acta [Wien] 1, 255–258.
15 Becker, A., Taran, Ch., Uhmann, W. and Siebert, F. (1989) in Proceedings of Seventh International Conference On Fourier and Computerized Infrared Spectroscopy (Cameron, D., ed.), pp. 512–513, SPIE, Bellingham WA.
16 Thibodeau, D.L., Breton, J., Berthomieu, C., Bagley, K.A. Mäntele, W. and Nabedryk, E. (1990) in Reaction Centres of Photosynthetic Bacteria; Structure and Dynamics (Michel-Beyerle, M.E., ed.), Springer, Berlin, in press.
17 Wraight, C.A. (1977) Biochim. Biophys. Acta 459, 525–531.
18 Griffiths, P.R., Foskett, C.T and Curbello, R. (1972) Appl. Spectr. Rev. 6, 31–78.
19 Buchanan, S., Michel, H. and Gerwert, K. (1990) in Current Research in Photosynthesis, (Baltscheffsky M., ed.), Kluwer Academic Publishers, Dordrecht, Vol. I, pp. 69–72.
20 Warncke, K. and Dutton, P.L. (1990) Biophys. J. 57, 571a.
21 Feher, G., Isaacson, R.A., Okamura, M.Y. and Lubitz, W. (1985) in Antennas and Reaction Centers of Photosynthetic Bacteria (Michel-Beyerle, M.E., ed.), pp. 174–189, Springer, Berlin.
22 Mäntele, W., Leonhard, M., Bauscher, M., Nabedryk, E., Breton, J. and Moss, D. (1990) in Reaction Centres of Photosynthetic Bacteria: Structure and Dynamics (Michel-Beyerle, M.E., ed.), Springer, Berlin, in press.
23 Berthomieu, C., Nabedryk, E., Mäntele, W. and Breton, J. (1990) FEBS Lett. 269, 00–00.
24 Trebst, A. (1986) Z. Naturforsch., C:Biosci. 41C, 240–245.
25 Michel, H. and Deisenhofer, J. (1988) Biochemistry 27, 1–7.
26 Mäntele, W., Hienerwadel, R., Lenz, F., Riedel, W.J., Grisar, R. and Tacke, M. (1990) Spectr. Int., in press..